Regional-Scale Lithospheric Recycling on Venus via Peel-Back Delamination

Andrea C. Adams[1]*, Dave R. Stegman[1], Suzanne E. Smrekar[2], Paul J. Tackley[3]

[1]Institute of Geophysics and Planetary Physics, Scripps Institution of Oceanography, University of California, San Diego
[2]Jet Propulsion Laboratory, California Institute of Technology, Pasadena, CA, USA
[3]Institute of Geophysics, Department of Earth Sciences, ETH Zürich, Zürich, Switzerland
*aca009@ucsd.edu

Jet Propulsion Laboratory
California Institute of Technology

20th Meeting of the Venus Exploration Analysis Group (VEXAG)
7-9 November 2022

Introduction

- Over 10,000 km of possible subduction sites have been identified on Venus, which have elastic thicknesses, plate bending moments and bending curvatures comparable to subduction zones on Earth (Schubert & Sandwell, 1995).
- Proposed subduction sites are located near (1) coronae and (2) groupings of rift-zone trenches called chasmata (Fig. 1).
- Previous numerical (Gülcher et al., 2020) and experimental (Davaille et al., 2017) studies have validated the possibility of regional-scale subduction initiation at coronae via plume-lithosphere interactions.
- Until now, no studies have tested the viability of subduction initiation at a chasma rift zone on Venus.

Here, we present numerical experiments used to determine if and how regional-scale lithospheric recycling could be initiated at a Venusian rift zone.

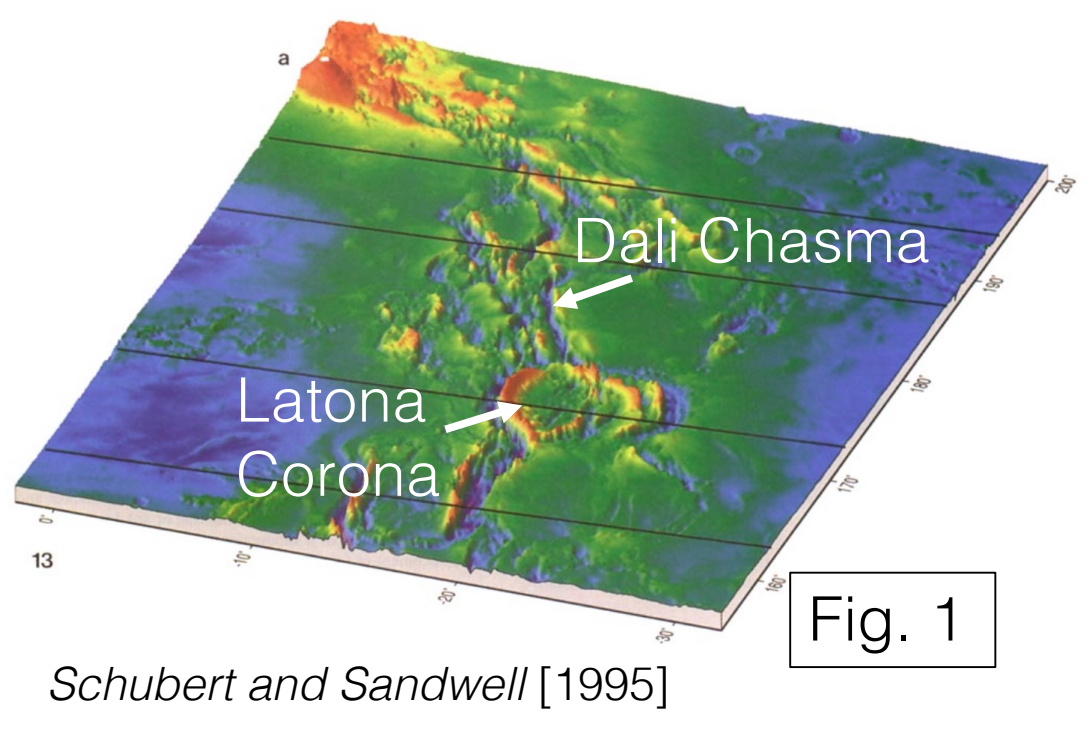

Schubert and Sandwell [1995]

Fig. 1

Model Setup

- 2D spherical annulus numerical models using StagYY (Tackley, 2008)
- Parameter space:
  - Lithosphere thickness, h_L = [200, 250, 300] km
  - Maximum viscosity, η_{max} = [10^{23}, 10^{24}, 10^{25}] Pa·s
  - Compositional buoyancy of crust (i.e. $B_{crust} = \rho_{0,crust} - \rho_{0,mantle}$)
    B_{crust} = [-175, -265, -300, -350, -400] kg/m^3
- Earth-like phase transitions were adjusted to shallower depths due to Venus's lower gravity (Ogawa & Yanagisawa, 2014) (Fig. 3)
- Post-processing and visualization done using StagLab (Crameri, 2018)

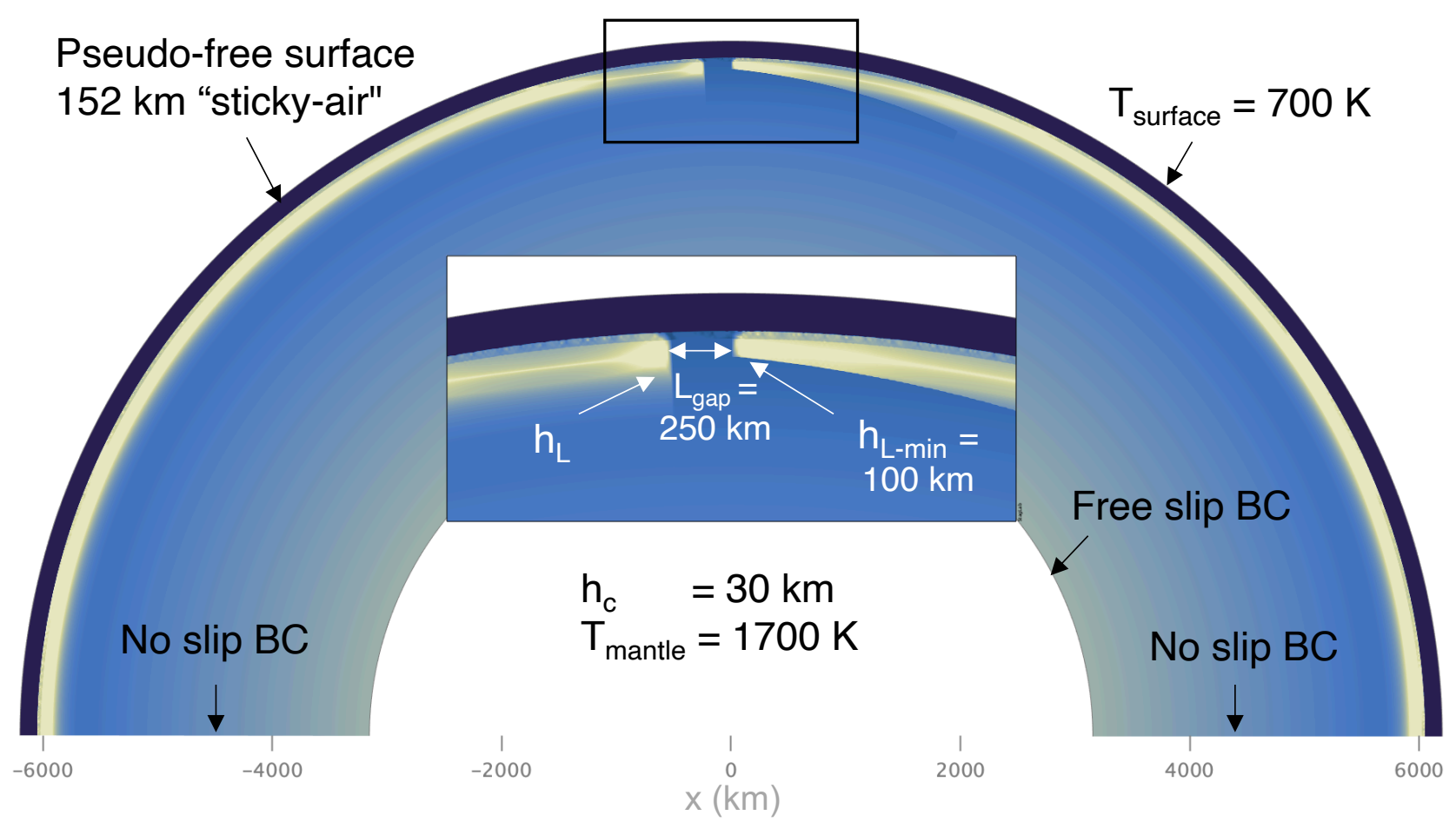

Fig. 2

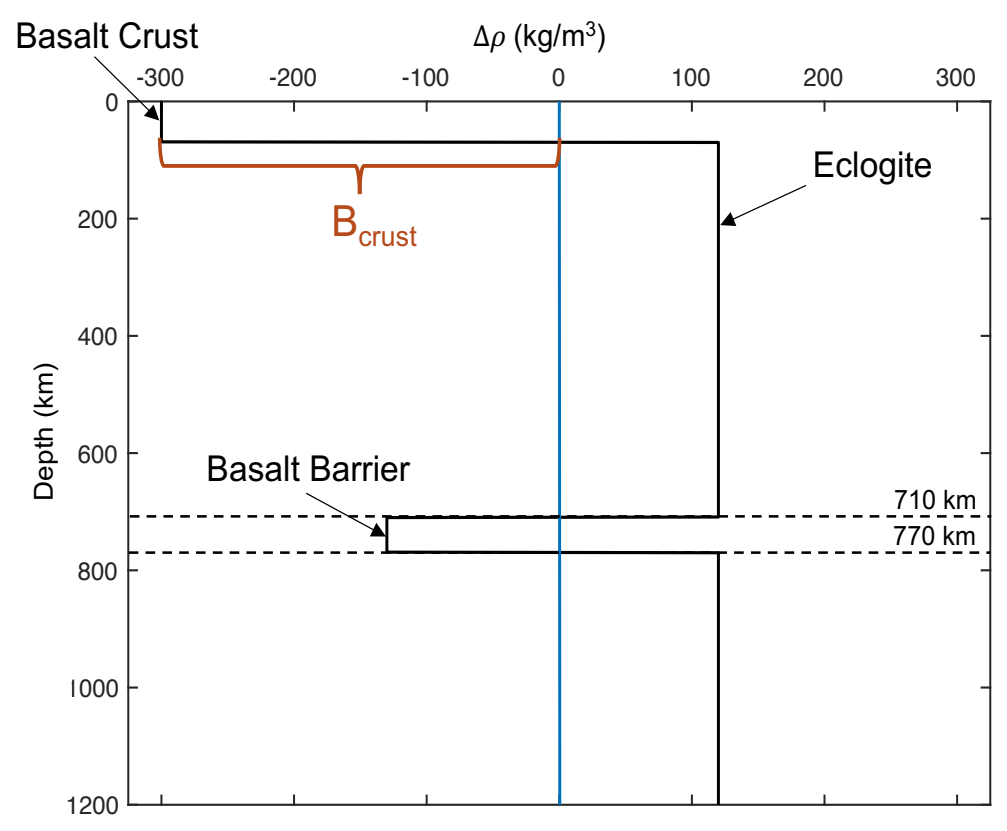

Fig. 3: Phase Transitions

Peel-Back Delamination

- All lithospheric recycling events occurred via the peel-back delamination tectonic regime.
- *Peel-back delamination* is a form of lithospheric recycling which occurs when dense lithospheric mantle decouples from the crust and peels away, leaving behind a hot, thinned layer of crust at the surface.

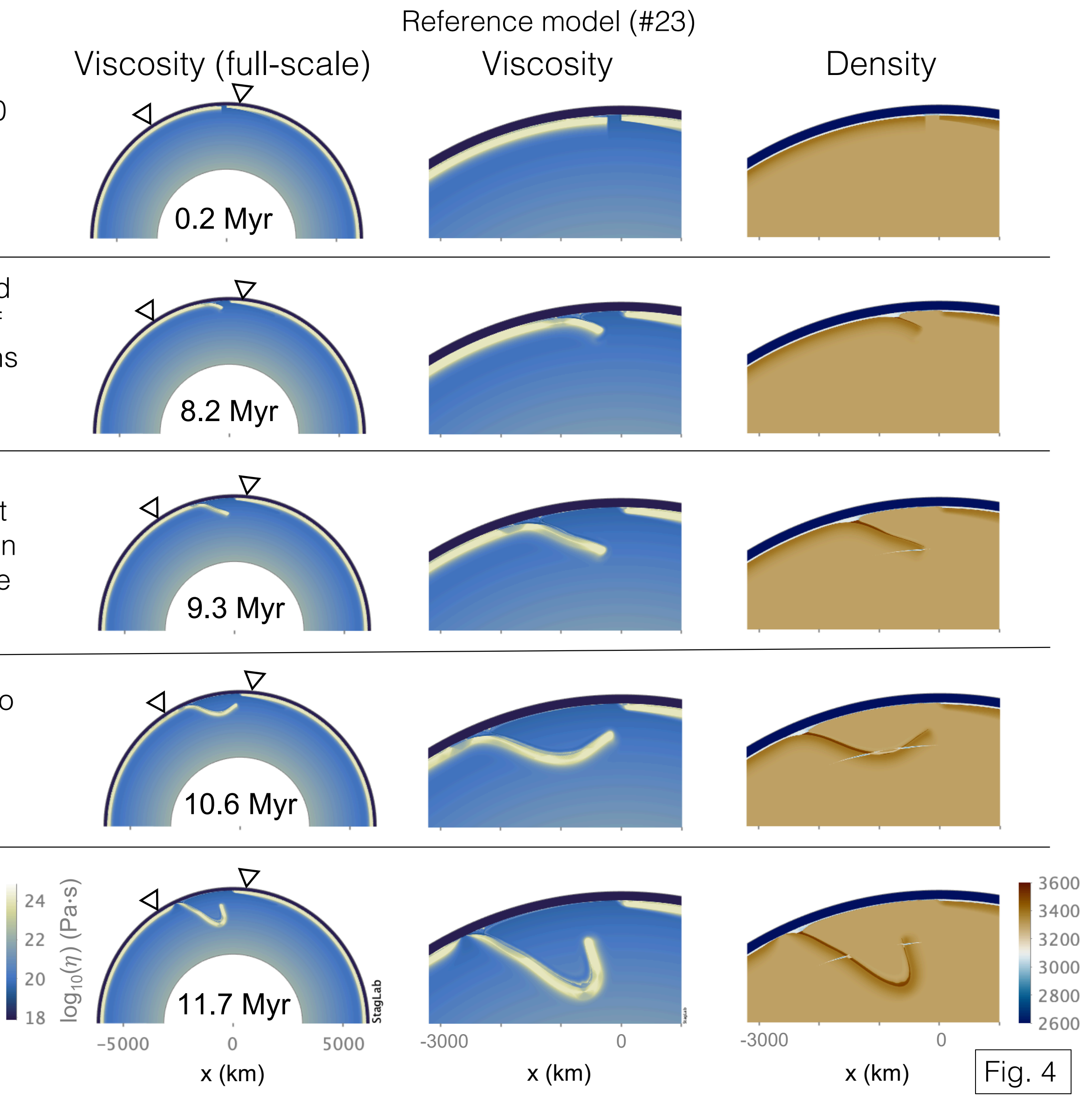

A Ref. model (#23) with B_{crust} = -300 kg/m^3, h_L = 250 km, η_{max} = 10^{24} Pa·s.

B Thicker plate edge begins to bend downward due to (-) buoyancy of lithospheric mantle. Eclogite begins to form.

C The slab peels back from the surface and thicker layers of crust are subducted due to eclogitization of the crustal root. Crust over plate gap continues to be thinned.

D Slab tip is deflected upward due to positive buoyancy of the garnet trap and postspinel phase boundary deflection.

E The plate necks and thins at the delamination hinge prior to slab break-off at the surface

Fig. 4

Mechanism for Delamination Initiation

- 30 km-thick layer of crust is relatively weak (C_0 = 10 MPa).
- Excess negative buoyancy of the lithospheric mantle results in initial plate bending, which causes the crust to yield (Fig. 5A)
- Crustal yielding reduces its viscosity, creating a weak-zone delamination-surface to enable decoupling of the crust and lithospheric mantle.
- The length of the weak zone increases with increasing plate bending and crustal yielding (Fig. 5C).
- Eclogite formation at the base of crustal root (~70 km depth) helps sustain slab sinking (Fig. 5F, 5H).

Thicker, more negatively-buoyant lithosphere enhances crustal yielding and weak-zone formation, which enables delamination initiation.

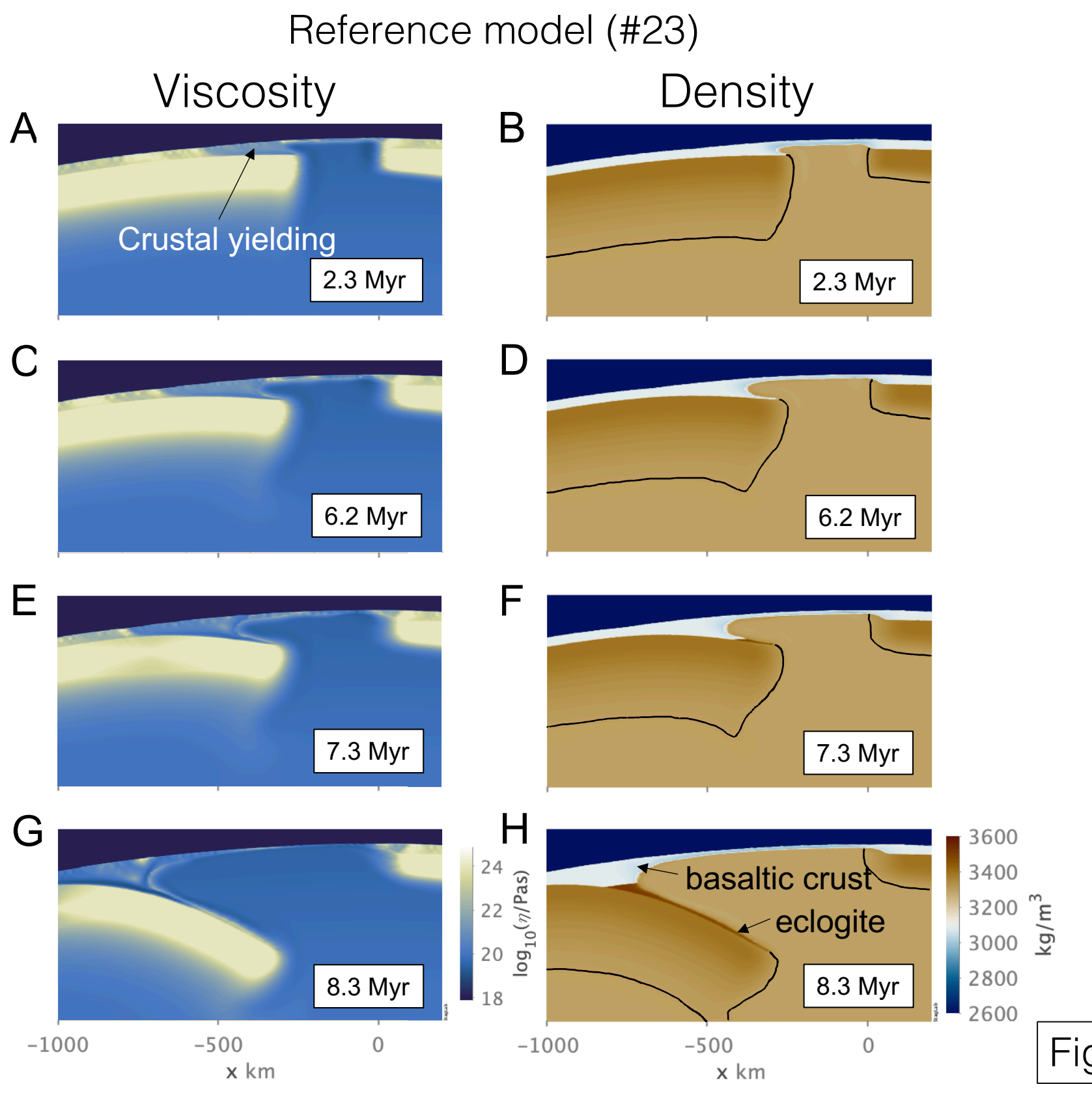

Fig. 5

Calculating Plate Buoyancy

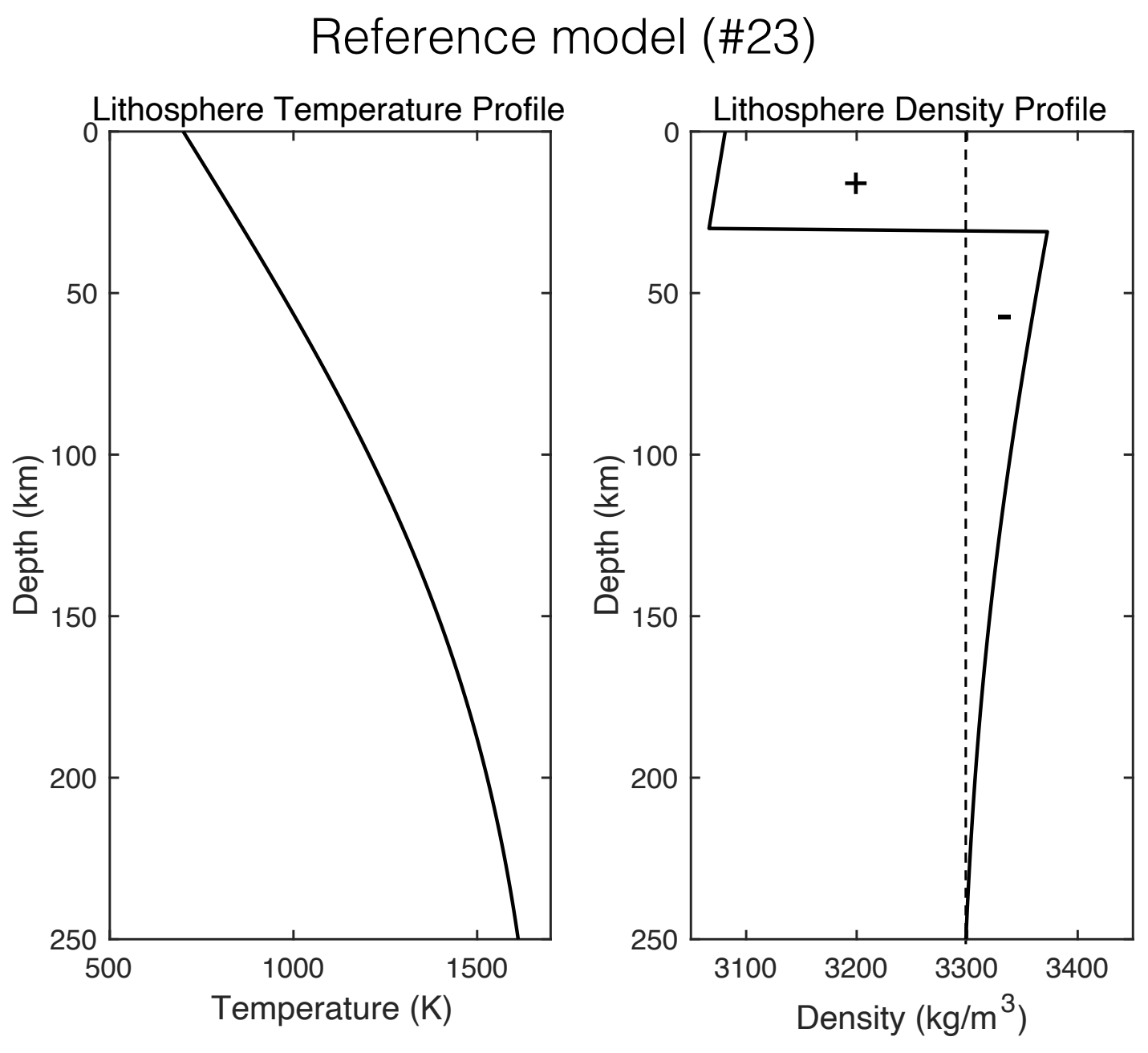

Fig. 6

- Net plate buoyancy was controlled by two of the three variables in our parameter space: lithosphere thickness and crust density.
- The total density of each plate was calculated as a function of depth, including both thermal and compositional components (Fig. 6).
- Integrating the density profiles over depth with respect to the reference mantle density gives a single value, $\Delta\rho_{plate}$, describing the net density contrast between the plate and the underlying mantle:

$$\Delta\rho_{plate} = \int_0^{h_L} (\rho(z) - \rho_0)dz$$

Tectonic Regime Diagram

- Only two tectonic regimes were observed: stagnant-lid (S.L.) or peel-back delamination.
- All negatively-buoyant plates delaminated, but not all positively-buoyant plates remained S.L.
- For positively-buoyant plates:
  - Thickest lithosphere (300 km) always delaminated
  - Thinnest lithosphere (200 km) remained S.L.
  - Increasing crustal buoyancy caused 250 km-thick plate to go from delamination to S.L.

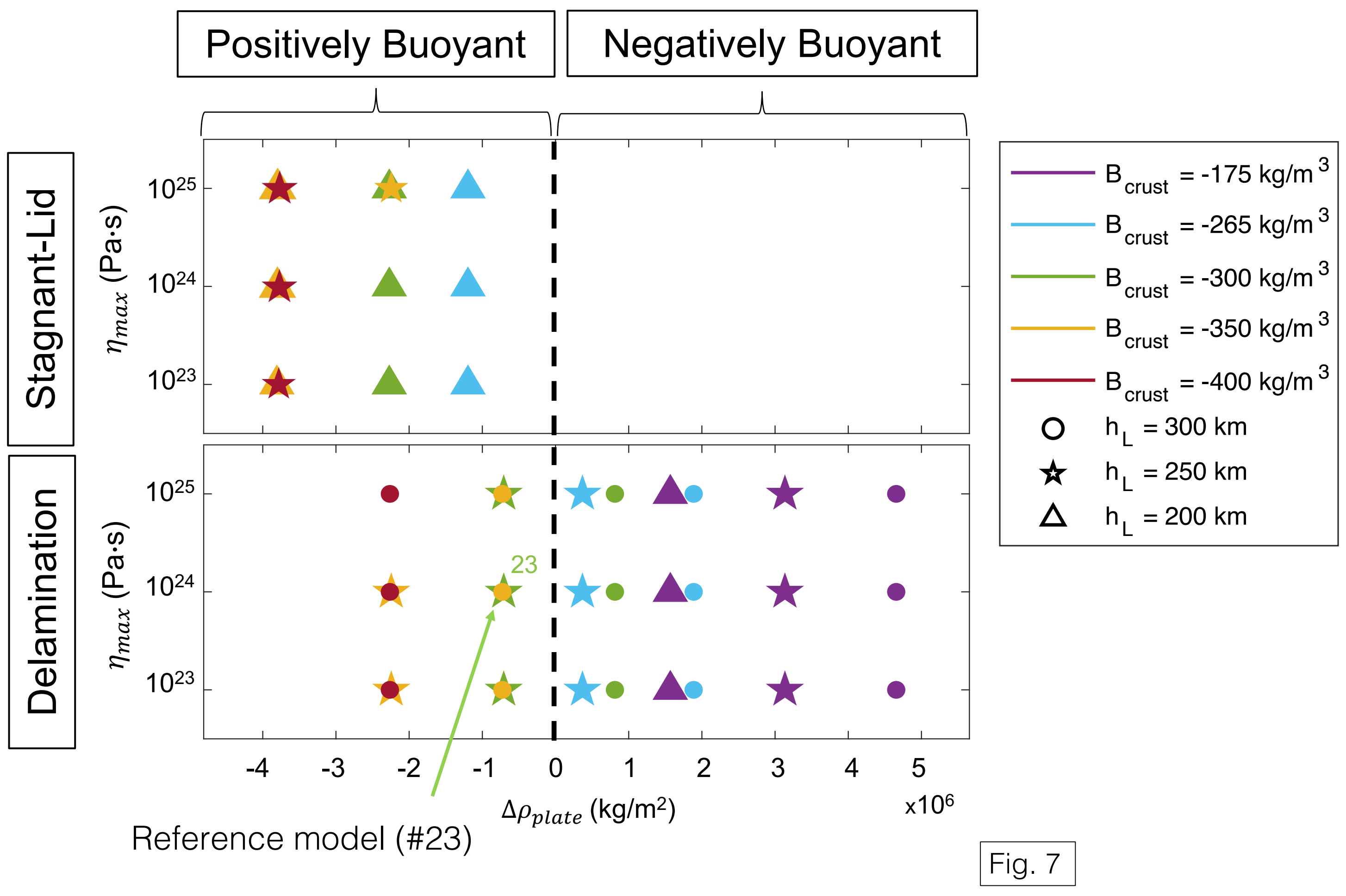

Fig. 7

Conclusions

- Peel-back delamination is driven by the negative buoyancy of the lithospheric mantle.
- Delamination is resisted by (1) the coupling of the plate across the Moho, (2) the positive compositional buoyancy of the crust, and (3) increasing plate strength.
- Unlike subduction, delamination does not require net-negative plate buoyancy.
- Following a delamination event, the emplacement of hot, buoyant asthenosphere beneath the crust may have consequences for regional-scale volcanism and tectonic deformation.

References

- Crameri, F. "Geodynamic diagnostics, scientific visualization and StagLab 3.0." Geoscientific Model Development 11.6 (2018).
- Davaille, A., Smrekar, S. E., and Tomlinson, S. (2017). Experimental and observational evidence for plume-induced subduction on venus. *Nature Geoscience, 10,* 349-355.
- Gülcher, A. J., Gerya, T. V., Montési, L. G., and Munch, J. (2020). Corona structures driven by plume-lithosphere interactions and evidence for on-going plume activity on venus. *Nature Geoscience*, *13*, 547-554.
- Schubert, G. and Sandwell, D. T. "A global survey of possible subduction sites on Venus." Icarus 117 (1995):173-196.
- Tackley, Paul J. "Modelling compressible mantle convection with large viscosity contrasts in a three-dimensional spherical shell using the yin-yang grid." Physics of the Earth and Planetary Interiors 171. 1-4 (2008): 7-18.

Acknowledgements

The authors are grateful for support from NASA Award 80NSSC22K0100. Computational resources were provided by Extreme Science and Engineering Discovery Environment (XSEDE), which is supported by National Science Foundation grant number ACI-1053575. The authors would like to thank David Sandwell for helpful discussions.